Updated measurements of [OIII]88μm, [CII]158μm, and dust continuum emission from a z =7.2 galaxy

Yi W. Ren, Yoshinobu Fudamoto, Akio K. Inoue, Yuma Sugahara, Tsuyoshi Tokuoka, Yoichi Tamura, Hiroshi Matsuo, Kotaro Kohno, Hideki Umehata, Takuya Hashimoto, Rychard Bouwens, Renske Smit, Nobunari Kashikawa, Takashi Okamoto, Takatoshi Shibuya, Ikkoh Shimizu

Galaxy-IGM workshop 2022

INTRODUCTION

- Observe galaxies in the reionization epoch:
  - Understand the galaxy evolution
  - Understand the reionization process, etc.
- [OIII] 88 μm emission line:
  - $^3P_1 \rightarrow {}^3P_0$ transition of O^{2+}, arising from H II regions
- [CII] 158 μm emission line:
  - $^2P_{3/2} \rightarrow {}^2P_{1/2}$ transition of C^+, arising from diffuse H I clouds, PDRs, etc.
- Dust continuum emission: thermal emission re-emitted by dust after absorbing stellar radiation
- Emission can provide information about star-formation process and interstellar medium (ISM), like gas density, metallicity, etc.

Credit: Amanda Smith, Institute of Astronomy

INTRODUCTION

- **Target:**
  - SXDF-NB1006-2 at z= 7.212
  - forbidden emission lines: [OIII] 88 μm, [CII] 158 μm
  - Dust continuum emission
- **Tool:** Atacama Large Millimeter/submillimeter Array (ALMA)
- **Previous studies:**
  - Inoue et al. 2016:
    - [OIII]88μm :
      - 5.3σ, Cycle 2 (2013.1.01010.S)
    - [CII]158μm :
      - Non-detection, Cycle 1 (2012.1.00374.S)
    - Dust continuum: non-detection
  - Carniani et al. 2020:
    - [CII]158μm :
      - 4.1σ Cycle 1 + Cycle 3 (2013.A.00021.S)

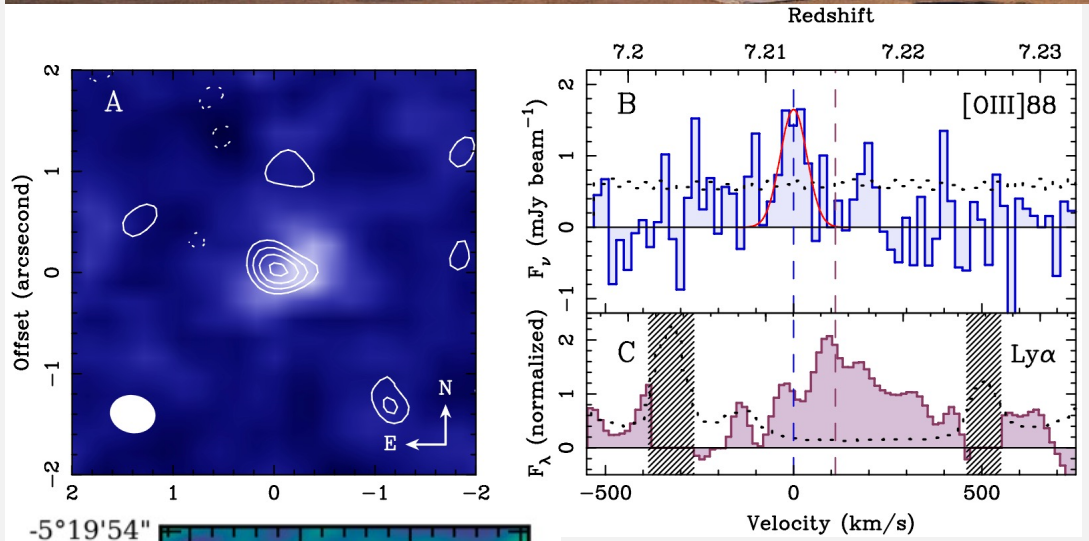

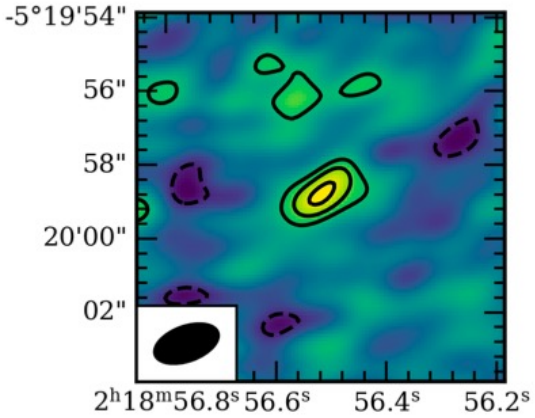

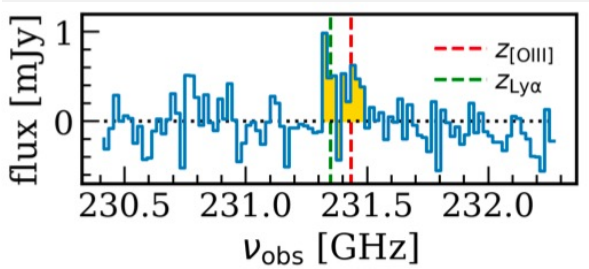

DATA

- The Common Astronomy Software Application (CASA)
  - **Statwt**: correct visibility weights of Cycle 1 [CII] data before combining it with other data
  - **Tclean**: dirty images
  - **Immoments**: integrated intensity maps
  - **Imfit**: integrated flux density, intrinsic size, coordinate
  - **Specfit**: gaussian fitting

Table 1. Summary of the observations used in this work

	Cycle Number	Project ID	Angular Resolution*	$\sigma^{\dagger}$ mJy/beam
[OIII] 88 μm	2	2013.1.01010.S	$0.45'' \times 0.38''$	0.23
	3	2015.A.00018.S	$0.135'' \times 0.128''$	0.13
[CII] 158 μm	1	2012.1.00374.S	$0.8'' \times 0.6''$	0.11
	3	2013.A.00021.S	$1.9'' \times 1.0''$	0.12
	7	2019.1.01634.L	$1.5'' \times 1.2''$	0.18

NOTE—* Beam sizes of the moment-0 maps with natural weighting. † RMS of images with bin width of 100 km/s.

New in this work

REBELS large program

RESULT-[OIII]88μm

- Cycle 2:
  - Beam size: 0.45″×0.38″
  - Rms: 0.064 Jy/beam·km/s
- Cycle 3:
  - Clumpy structure
  - Beam size: 0.135″×0.128″
  - Rms: 0.0335 Jy/beam·km/s
  - A+B: 0.422±0.144 Jy·km/s
  - A+B+C: 0.643±0.170 Jy·km/s

Table 2. Summary of the SNRs and flux densities of Cycle 2, Cycle 3 and Cycle 2+3 [OIII] 88 μm data.

	SNR	Integrated Flux (Jy km/s)	Major/minor axis FWHMs (″)
Cycle 2	5.2/5.3*	0.446 ± 0.137 / 0.45 ± 0.09*	0.30 ± 0.20 × 0.14 ± 0.12
Cycle 2+3	5.8	0.578 ± 0.154	0.57 ± 0.19 × 0.38 ± 0.16
Cycle 3 A	3.2	0.198 ± 0.091	0.17 ± 0.09 × 0.04 ± 0.08
Cycle 3 B	3.3	0.224 ± 0.112	0.24 ± 0.13 × 0.07 ± 0.08
Cycle 3 C	3.8	0.221 ± 0.090	0.33 × 0.056

NOTE—* Values are from Inoue et al. (2016). The results of Cycle 2+3 data is from image with 0.3″ uv-taper.

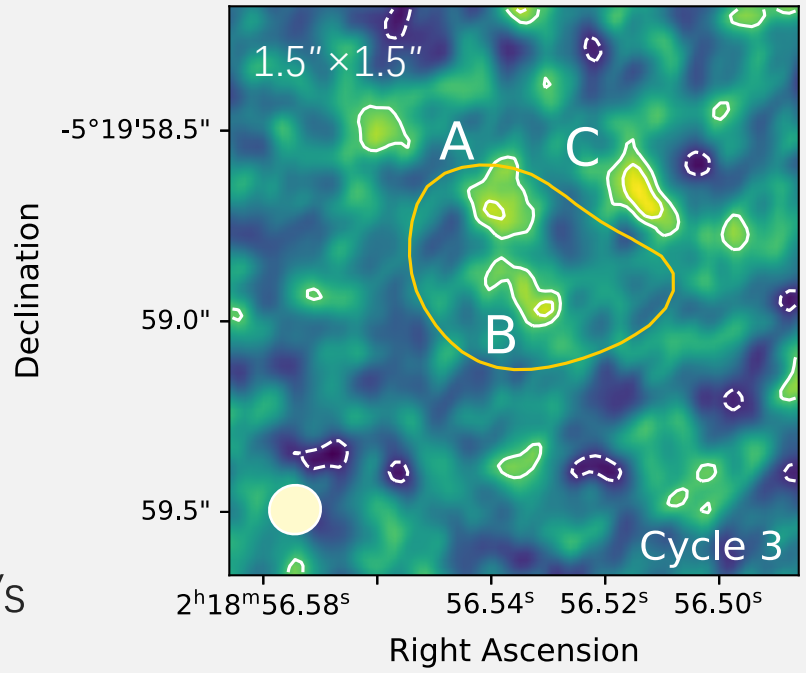

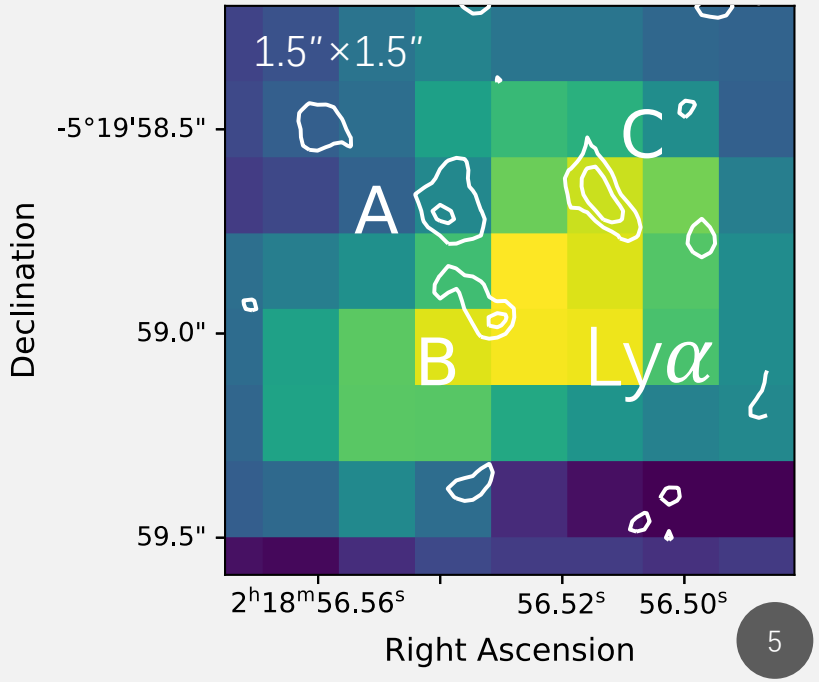

RESULT-[OIII]88μm

- Cycle 2 + Cycle 3 (uv-taper: 0.3″):
  - Beam size: 0.39″×0.34″
  - Rms: 0.0415 Jy/beam·km/s

Table 2. Summary of the SNRs and flux densities of Cycle 2, Cycle 3 and Cycle 2+3 [OIII] 88 μm data.

	SNR	Integrated Flux (Jy km/s)	Major/minor axis FWHMs (″)
Cycle 2	5.2/5.3*	0.446 ± 0.137 / 0.45 ± 0.09*	0.30 ± 0.20 × 0.14 ± 0.12
Cycle 2+3	5.8	0.578 ± 0.154	0.57 ± 0.19 × 0.38 ± 0.16
Cycle 3 A	3.2	0.198 ± 0.091	0.17 ± 0.09 × 0.04 ± 0.08
Cycle 3 B	3.3	0.224 ± 0.112	0.24 ± 0.13 × 0.07 ± 0.08
Cycle 3 C	3.8	0.221 ± 0.090	0.33 × 0.056

NOTE—* Values are from Inoue et al. (2016). The results of Cycle 2+3 data is from image with 0.3″ uv-taper.

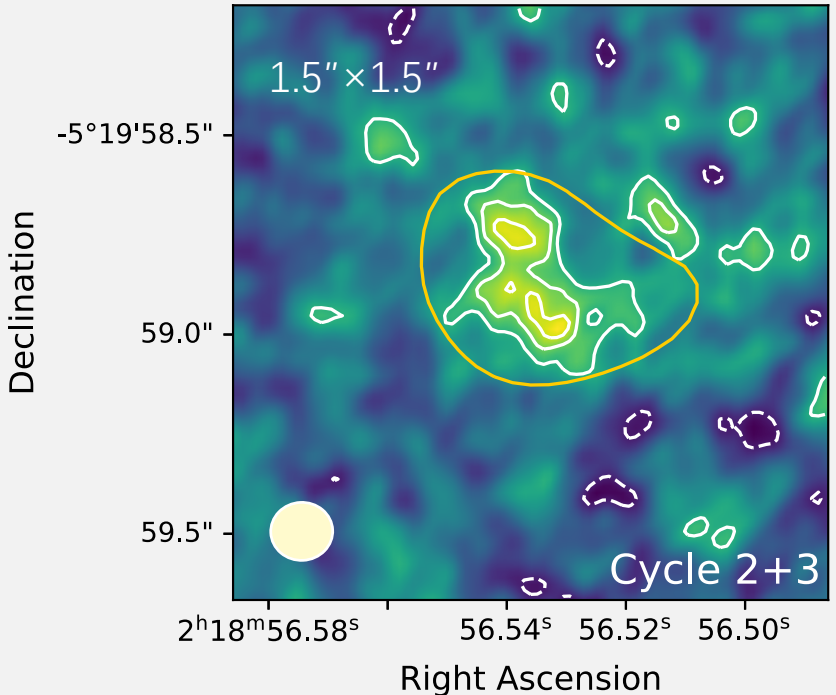

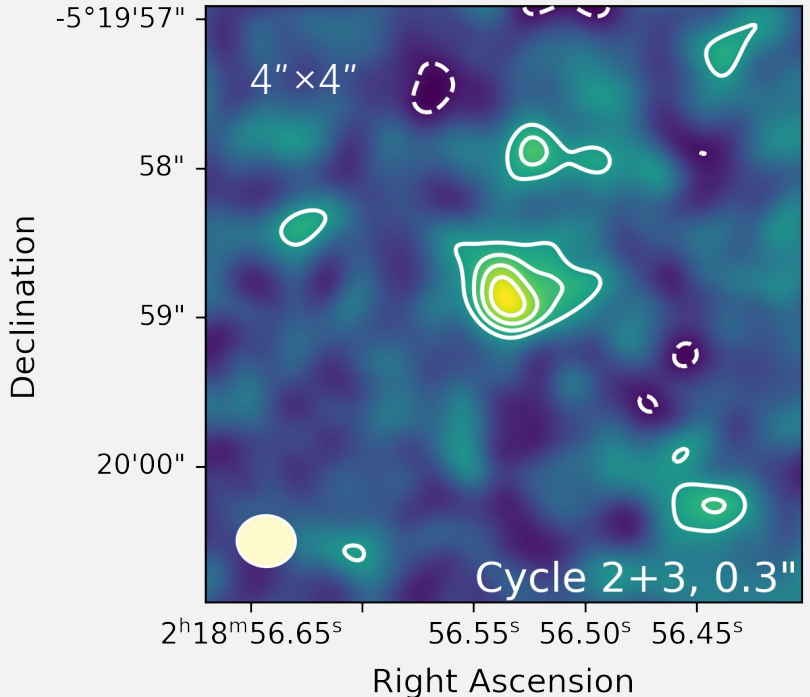

RESULT-[OIII]88μm

- Single beam spectral at peak position

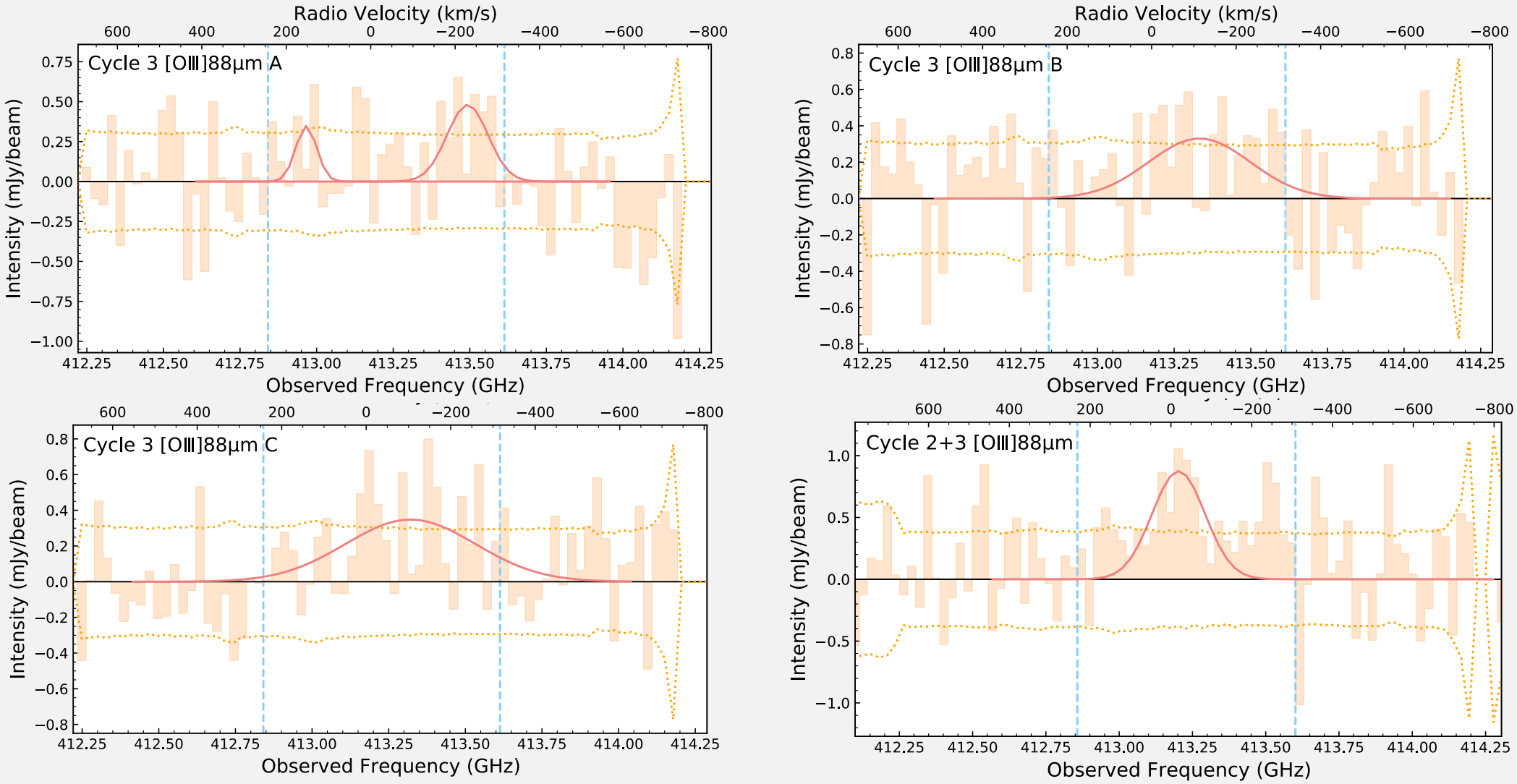

RESULT-[OIII]88μm

- Detailed integration-optimized detection
  - Cycle 2: 0.446±0.137 Jy·km/s
  - A1+A2+B*: 0.452±0.107 Jy·km/s (within 1σ)
  - A1+A2+B*+C*: 0.658±0.128 Jy·km/s (within 2σ)
  - A1+A2+B*+C**: 0.715±0.143 Jy·km/s (within 2σ)

	Integral Range (km/s)	RMS (Jy/beam·km/s)	SNR	Flux Density (Jy·km/s)
A1	-300 ~ -160	0.016	3.9	0.065±0.028
A2	0 ~ +240	0.023	4.3	0.161±0.070
B*	-320 ~ 0	0.025	4.3	0.226±0.076
C*	-280 ~ +20	0.024	4.5	0.206±0.071
C**	-280 ~ 240	0.032	4.2	0.263±0.095

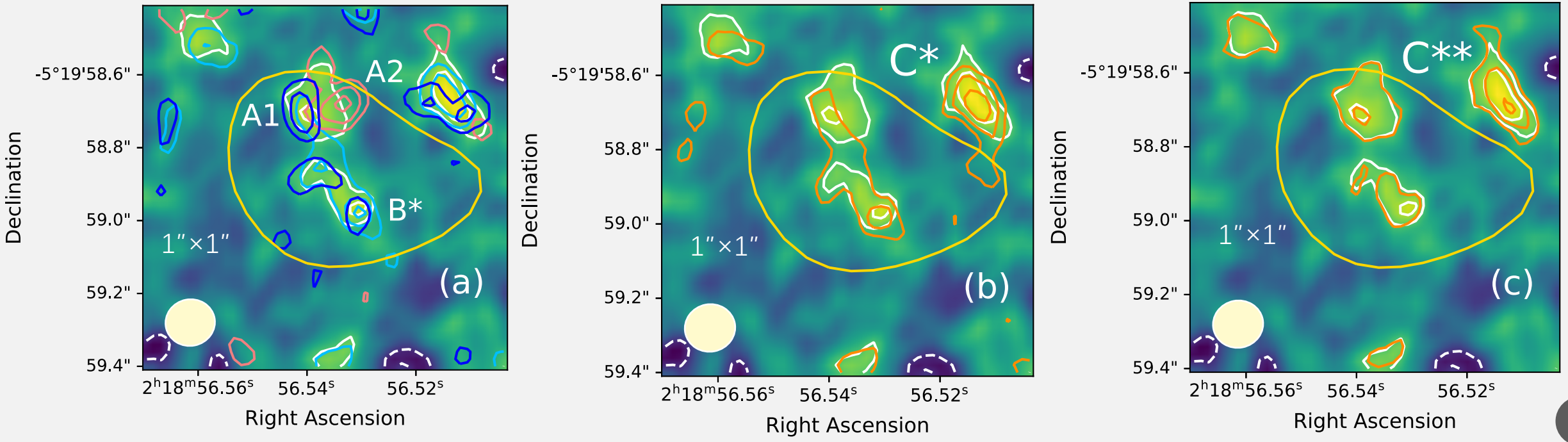

RESULT-[OIII]88μm

- Single beam spectral at peak position after detailed integration

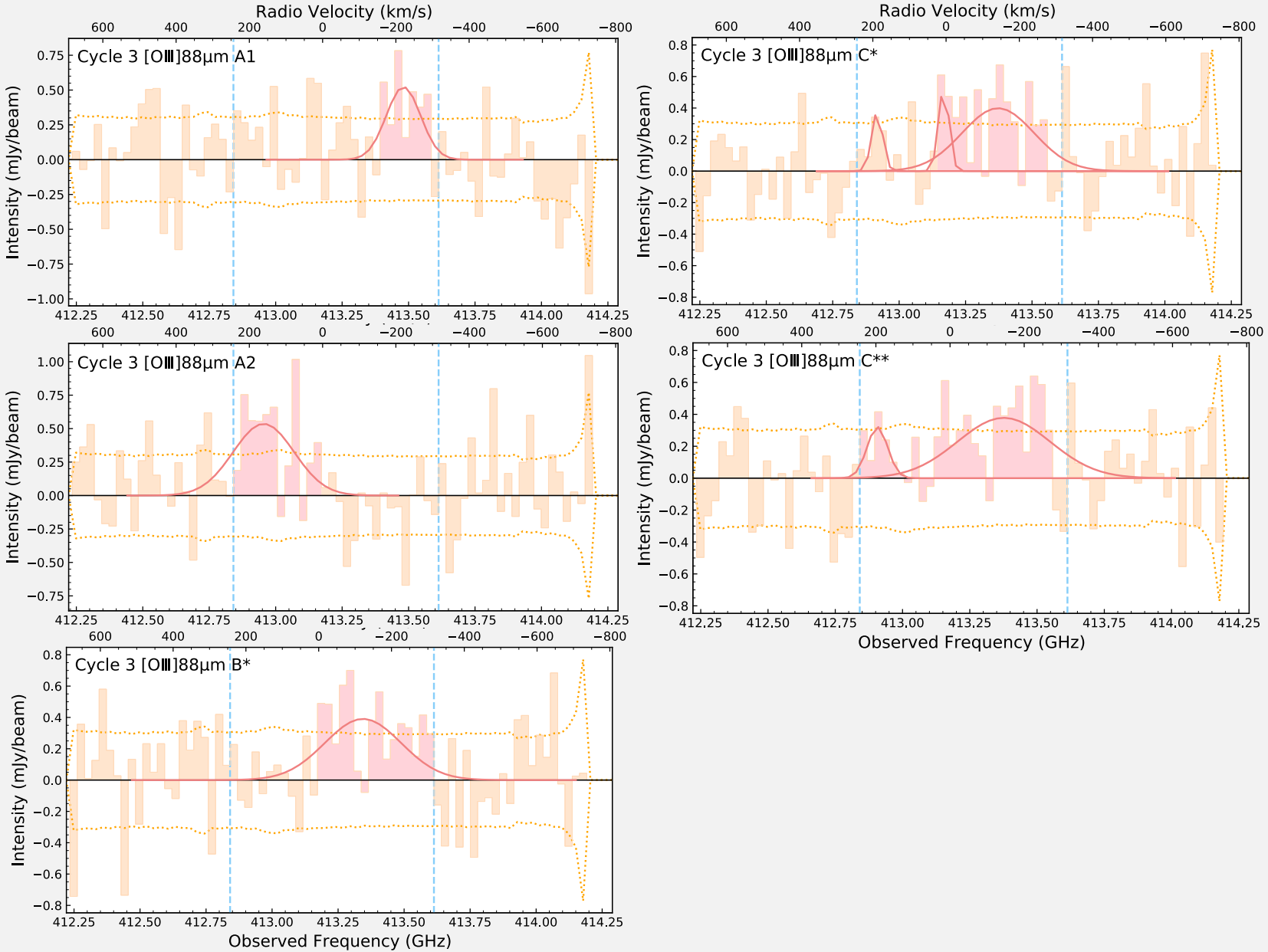

	Velocity Center (km/s)	Peak Intensity (mJy/beam)	FWHM (km/s)
0.3″ uv-taper			
Cycle 2	−0.9 ± 18.1	1.22 ± 0.23	157.4 ± 8.0
Cycle 2+3	−19 ± 17	0.875 ± 0.166	154.0 ± 8.6
A	153 ± 20	0.349 ± 0.248	58 ± 48
	−229 ± 19	0.481 ± 0.160	114 ± 44
A1	−221 ± 17	0.523 ± 0.167	110 ± 41
A2	161 ± 24	0.536 ± 0.139	196 ± 58
B	−113 ± 46	0.330 ± 0.107	284 ± 108
B*	−122 ± 34	0.391 ± 0.108	247 ± 80
C	−105 ± 45	0.348 ± 0.087	363 ± 106
C*	−142 ± 35	0.399 ± 0.105	231 ± 87
	188 ± 13	0.378 ± 0.288	35 ± 31
	6.2 ± 8.5	0.537 ± 0.329	33 ± 29
C**	−145 ± 35	0.378 ± 0.091	293 ± 84
	196 ± 20	0.322 ± 0.201	65 ± 48
[C II] 4.5 σ	42 ± 36	0.248 ± 0.075	−226 ± 83

RESULT-[CII]158μm

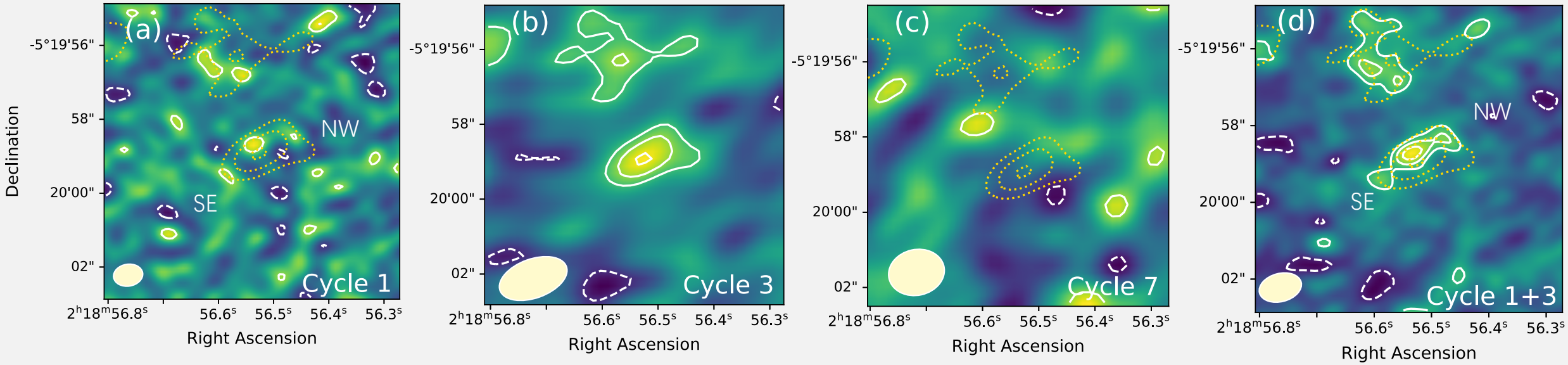

- Yellow dotted line in the images: 2σ, 3σ and 4σ contours of Cycle 3.
- There may be another 2 components, denoted by NW and SE.
- All the images above are images after excluding the effect of the atmospheric ozone line at ~231.28 GHz (v ~ 200 km/s).
- In the table, '-' denotes non-detection.

	Beam Size	RMS (Jy/beam·km/s)	SNR	Integrated Flux Density (Jy·km/s)	Major/minor axis FWHM (″)
Cycle 1	$0.8'' \times 0.6''$	0.017	3	0.028±0.014	-
Cycle 3	$1.9'' \times 1.0''$	0.024	4.2	0.134±0.051	$0.80 \pm 1.13 \times 0.62 \pm 0.28$
Cycle 7	$1.5'' \times 1.2''$	0.026	-	< 0.095 (< 0.084)† (3σ)	-
Cycle 1+3	$1.1'' \times 0.73''$	0.014	4.7	0.122±0.044	$2.03 \pm 0.98 \times 0.24 \pm 0.41$
Cycle 1+3+7	$1.2'' \times 0.77''$	0.013 (0.012)†	4.5 (3.3)†	0.125±0.043 (0.060±0.033)†	$2.20 \pm 1.00 \times 0.40 \pm 0.37$

NOTE—"-" means non-detection. † Results of integration without one peculiar bin at the integral edge.

RESULT-[CII]158μm

- Cycle 1+3+7 (a) 4.5 σ
- Cycle 1+3+7 (b), (c) show SE & NW clumps with optimized SNRs.
- In Cycle 1+3+7 (b), SNR~3.4;
- In Cycle 1+3+7 (c), SNR~3.2.
- FWHM: 226 ± 83 (km/s)

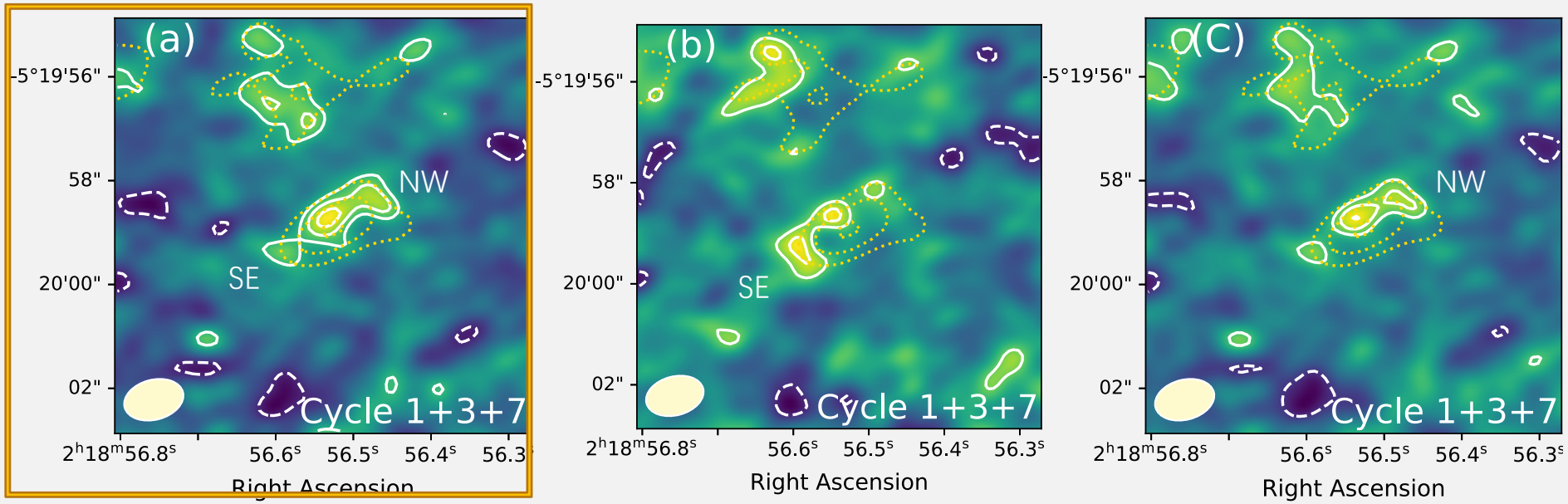

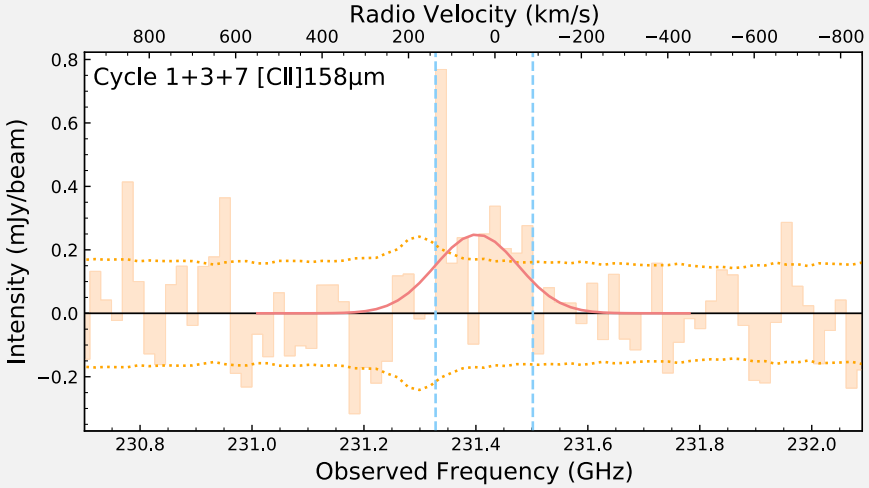

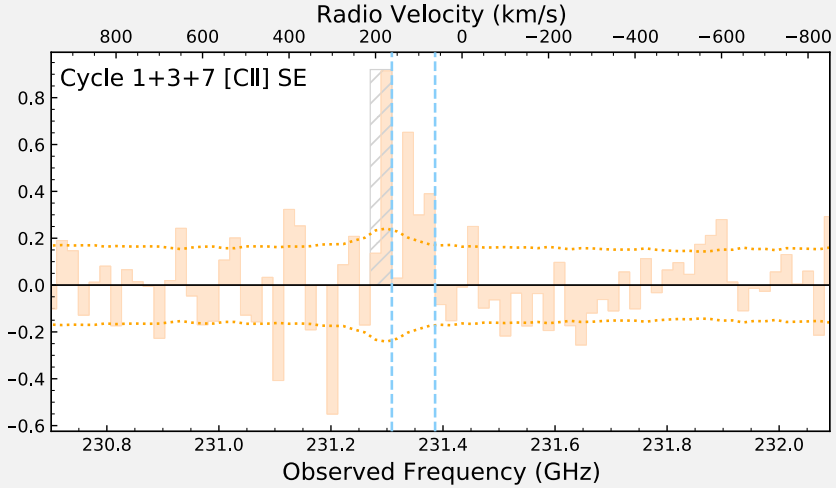

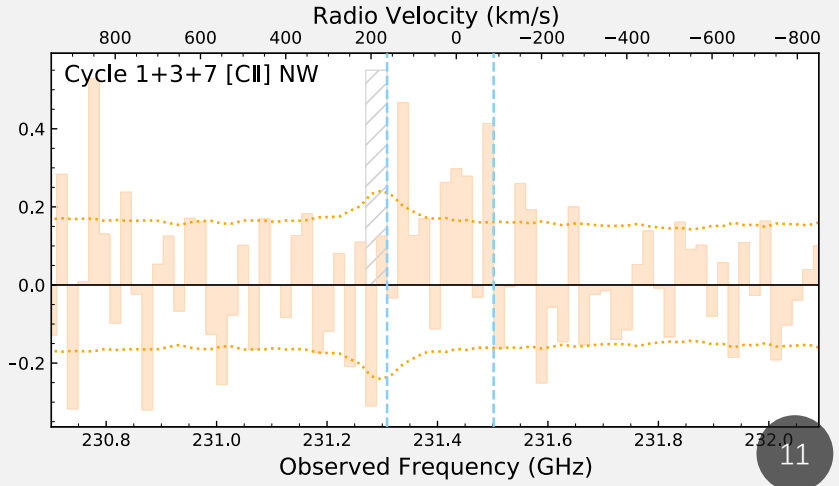

RESULT-[CII]158μm

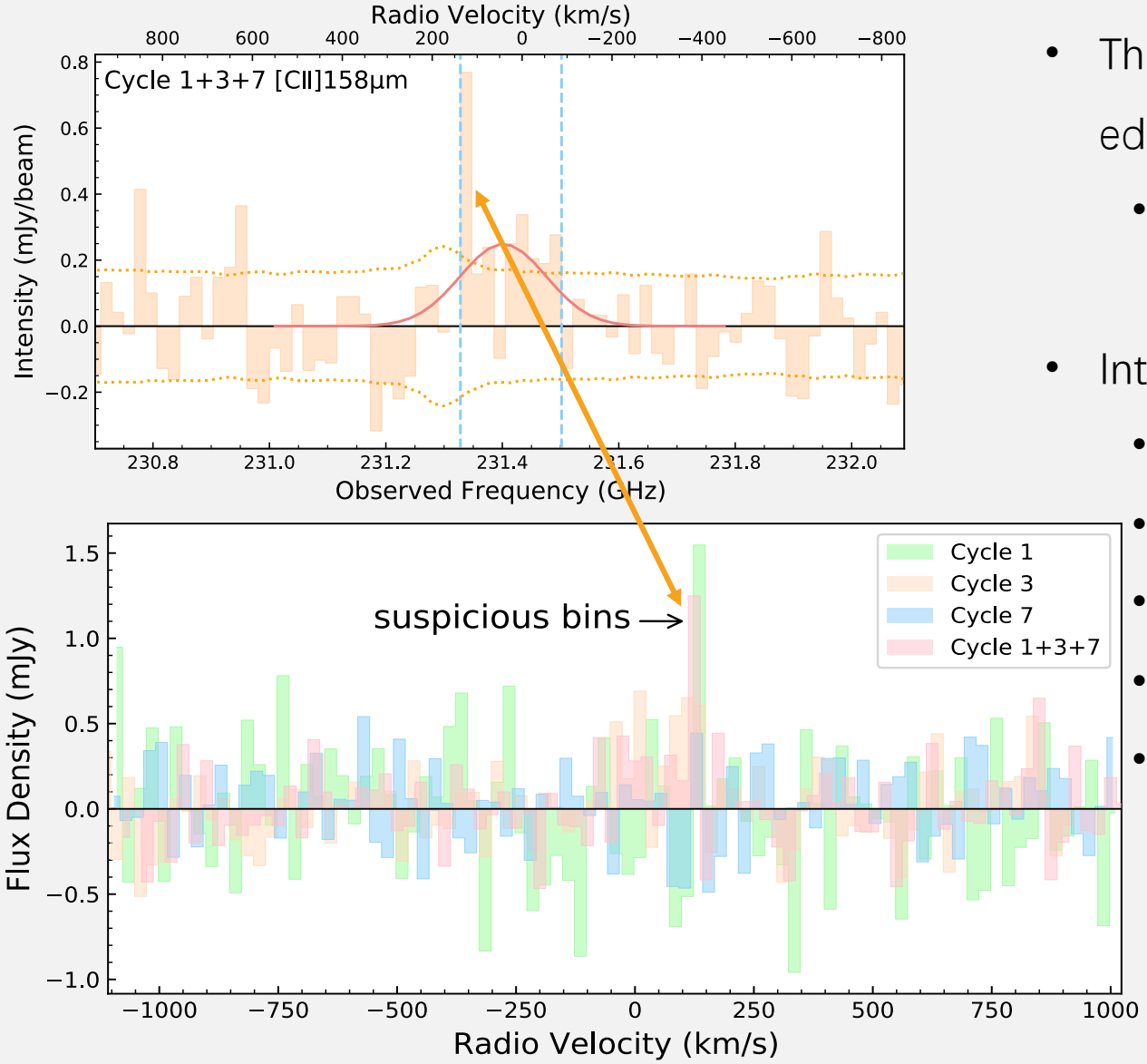

- There is a channel with particularly high intensity on the integral edge:
  - Affected by a suspicious spike on the spectrum of Cycle 1 (+110 km/s ~ +135 km/s)
- Integrate without this channel:
  - RMS: 0.013→0.012 Jy/beam·km/s
  - Integrated flux density: 0.125±0.043 → 0.060±0.033 Jy·km/s
  - SNR: 4.5σ →3.3σ
  - SE, NW < 3σ
  - size:

1.48″ ± 1.04″ × 0.21″ ± 0.65″

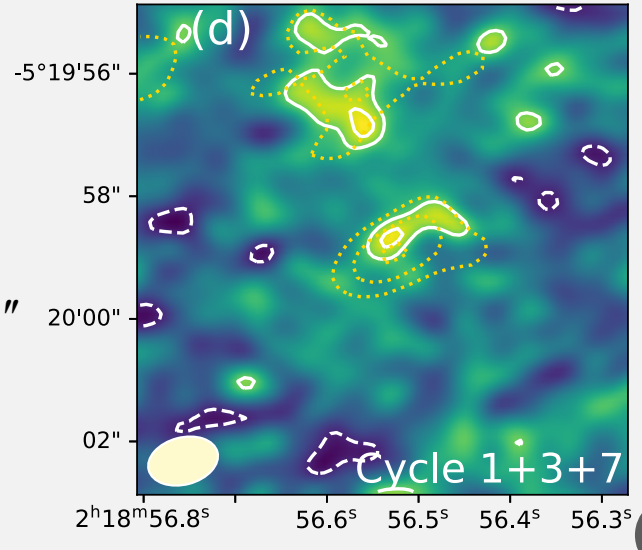

DUST CONTINUUM

- Dust continuum remains non-detection

Table 6. Measurements of dust continuum emission at Band 6 (1330 μm) and Band 8 (735 μm) and the upper limit on the dust infrared luminosity.

λ_{obs} (μm)	RMS (mJy/beam)	Flux Density (mJy)
735	0.0235	< 0.0705 ($3\,\sigma$)
1330	0.0095	< 0.028 ($3\,\sigma$)
IR luminosity (W)†	$< 2.1 \times 10^{37}$	(3σ)

† The dust temperature of 40 K and the emissivity index of 1.5 are assumed.

- Assume dust temperature = 40 k, emissivity index = 1.5 (Inoue et al. 2016), modified black body, integrate over 8-1000 μm:
  - Total Infrared luminosity < 2.1×10^{37} W (3σ)
  - Decreased by a factor of 1.38 than Inoue et al. 2016 (< 2.9×10^{37} W (3σ))

[OIII]/[CII] LUMINOSITY RATIO

	[O III] 88 μm*	[C II] 158 μm (4.5σ)†	[C II] 158 μm (3.3σ)‡
Integrated Flux (Jy·km/s)	0.578 ± 0.154	0.125 ± 0.043	0.060 ± 0.033
Flux ($W \cdot m^{-2}$)	$(8.0 \pm 2.1) \times 10^{-21}$	$(0.96 \pm 0.33) \times 10^{-21}$	$(0.46 \pm 0.25) \times 10^{-21}$
Luminosity (W)	$(4.9 \pm 1.3) \times 10^{35}$	$(0.59 \pm 0.20) \times 10^{35}$	$(0.28 \pm 0.15) \times 10^{35}$

- **[C II] 4.5σ:**
  - observed [OIII]/[CII]: **8.3 ± 3.6**
  - corrected for Surface Brightness Dimming (SBD) effect:
    - beam deconvolved source size: (2.20'' ± 1.00'') × (0.40'' ± 0.37'')
    - (θ_{beam}/D_{source}): 0.44±0.20
    - correction factor: 0.6±0.2
    - corrected [OIII]/[CII]: **5.0 ± 2.7**
- **[C II] 3.3σ:**
  - observed [OIII]/[CII]: **17.4 ± 10.4**
  - corrected for Surface Brightness Dimming (SBD) effect:
    - beam deconvolved source size: (1.48'' ± 1.04'') × (0.21'' ± 0.65'')
    - (θ_{beam}/D_{source}): 0.65±0.46
    - correction factor: 0.5±0.3
    - corrected [OIII]/[CII]: **8.7 ± 7.4**

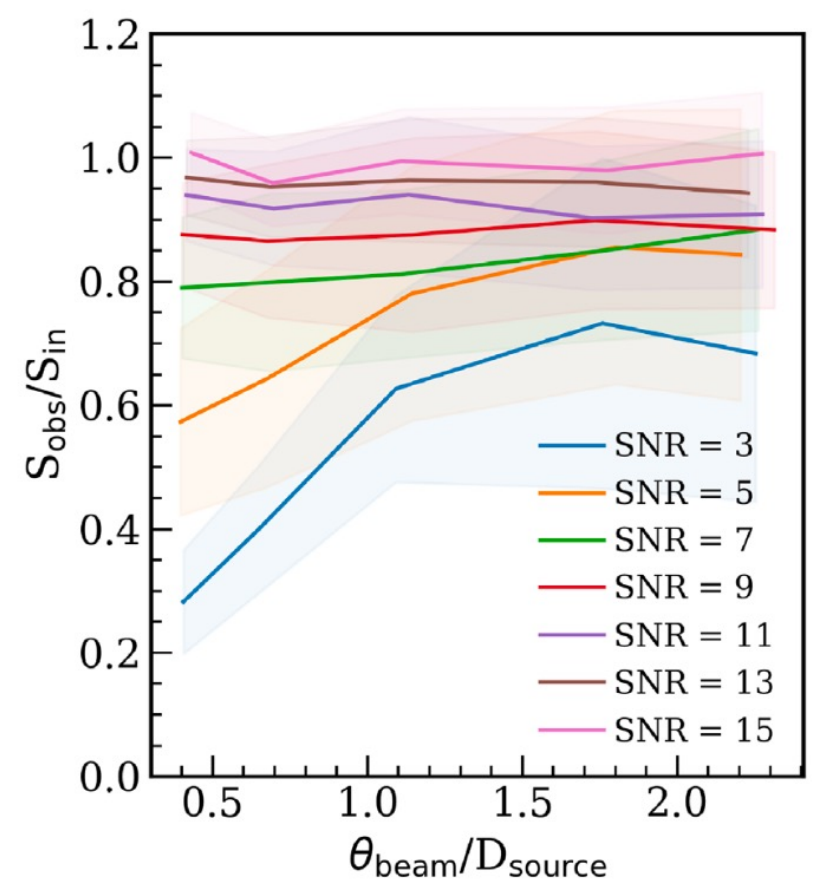

Figure 6 of Carniani et al. 2020

[CII]/SFR

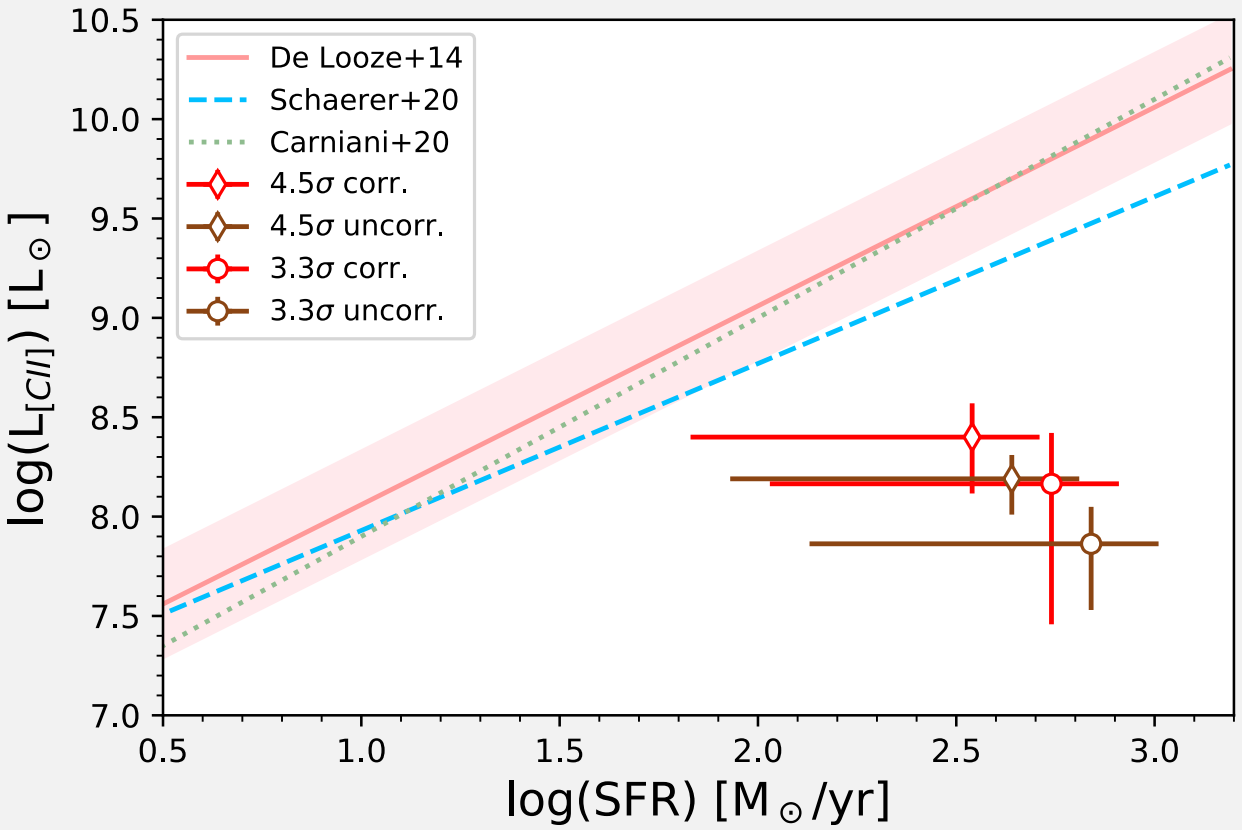

3 plots Lower are moved to the right one by one by 0.1 dex for display purpose.

- **Local** HII/starburst galaxy (De Looze+14):

  log SFR = (1.00 ± 0.04) log L[CII] − (7.06 ± 0.33)

- **4 < z < 6** star forming galaxy (Schaerer+20):

  log L[CII] = (0.84 ± 0.13) log SFR + (7.09 ± 0.21)

- **6 < z < 9** galaxy (Cariniani+20):

  log L[CII] = (1.1 ± 0.20) log SFR + (6.8 ± 0.2)

- Diamond: 4.5 σ
- Circle: 3.3 σ
- Our results are not consistent with any relation

SPATIAL DISTRIBUTION OF Lyα, [OIII] AND [CII]

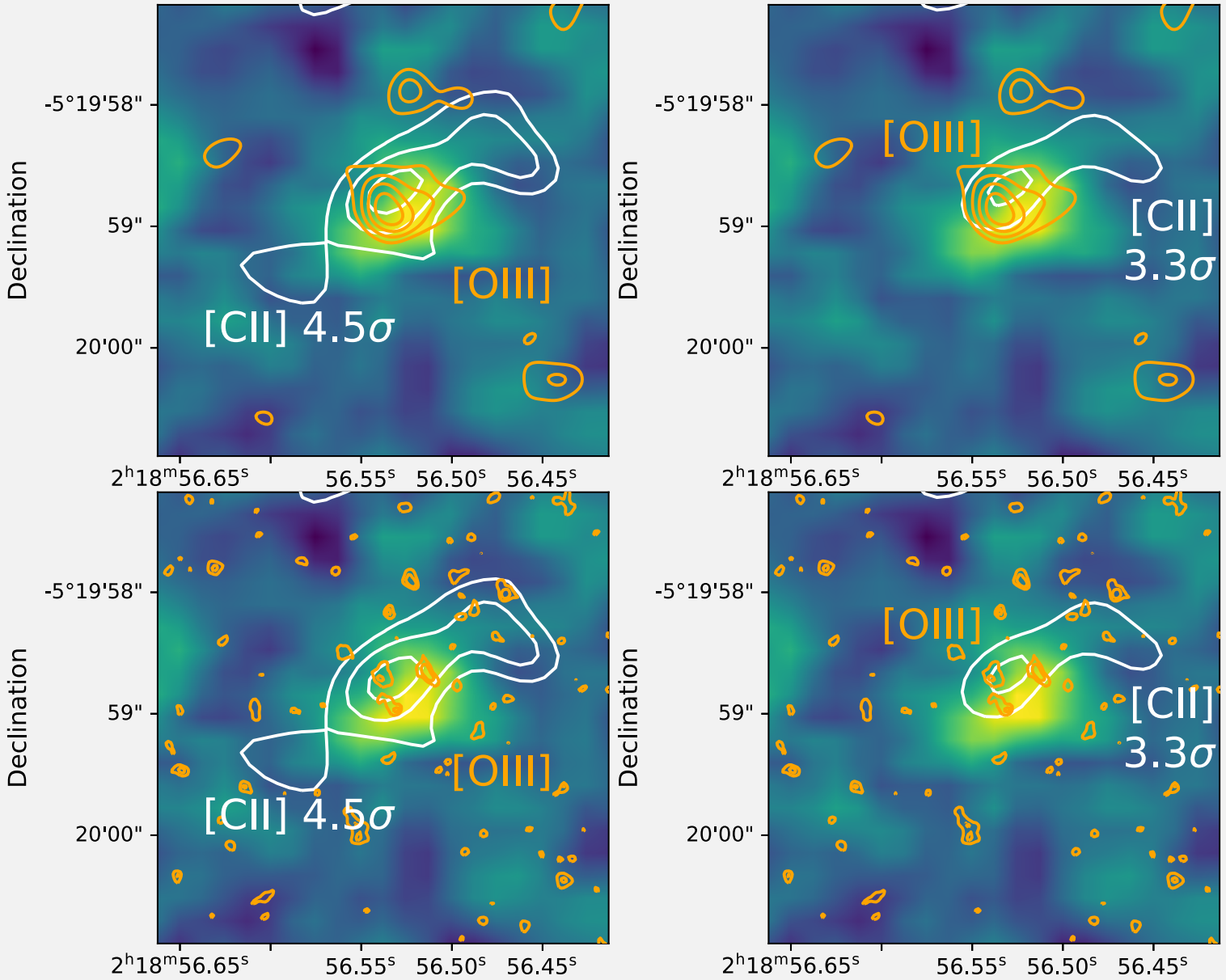

- [OIII] ~3σ clump: 0.42-0.70 kpc
- [OIII] 5.8σ: ~2.4 kpc
- [CII] 4.5σ: ~4.8 kpc
- [CII] 3.3σ: ~2.9 kpc

DISCUSSION AND SUMMARY

- [OIII] 88μm:
  - **Clumpy** structure.
  - Overall flux density including C becomes larger. Because It is consistent with Cycle 2 in 1σ (2σ) confidence level, **it is hard to determine if C is noise or not**.
  - **JWST** can confirm the clumpy structure.
- [CII] 158μm:
  - Marginal **4.5σ** detection, but the uncertainty in flux is very large. After removing the effect of systematic noise, the SNR significantly becomes small (**3.3σ**), so the **robustness of the detection is low**.
  - There may be another 2 components. Removing the effect of the atmospheric ozone line, optimized SNRs are 3.4σ and 3.2σ. But, after removing the effect of systematic noise, their SNRs < 3σ.
- Dust continuum:
  - Remains **non-detection**, indicating little dust fraction.
- [OIII]/[CII]:
  - **4 ratios**, consistent with local dwarf galaxies (0.5~11).
- [CII]/SFR:
  - Results are **not consistent** with any relation. The SFR may be overestimated. JWST can solve this problem.

	[C II] 158 μm	
	4.5 σ	3.3 σ
Observed [O III]/[C II] ratio	8.3 ± 3.6	17.4 ± 10.4
Beam size / [C II] size	0.44 ± 0.20	0.65 ± 0.46
SBD correction for [C II]†	0.6 ± 0.2	0.5 ± 0.3
Corrected [O III]/[C II] ratio	5.0 ± 2.7	8.7 ± 7.4